Breakdown current density of graphene nanoribbons

Raghunath Murali,[a] Yinxiao Yang, Kevin Brenner, Thomas Beck, and James D. Meindl
Microelectronics Research Center, Georgia Institute of Technology, Atlanta, Georgia 30332, USA

(Received 21 April 2009; accepted 1 May 2009; published online 19 June 2009)

Graphene nanoribbons (GNRs) with widths down to 16 nm have been characterized for their current-carrying capacity. It is found that GNRs exhibit an impressive breakdown current density, on the order of 10^8 A/cm^2. The breakdown current density is found to have a reciprocal relationship to GNR resistivity and the data fit points to Joule heating as the likely mechanism of breakdown. The superior current-carrying capacity of GNRs will be valuable for their application in on-chip electrical interconnects. The thermal conductivity of sub-20 nm graphene ribbons is found to be more than 1000 W/m K. © *2009 American Institute of Physics*. [DOI: 10.1063/1.3147183]

Graphene is a promising electronic material because of many interesting properties such as ballistic transport,[1] high intrinsic mobility,[2] and width-dependent band gap.[3] Graphene, in its two-dimensional (2D) form, has been shown to have a high thermal conductivity[4] of around 5000 W/m K pointing to its potential use as an on-chip heat spreader. Graphene nanoribbons (GNRs) have been predicted to be superior to Cu in terms of resistance per unit length[5] for use as on-chip interconnects. A high current-carrying capacity is critical for interconnect applications and reliability. There have been a number of studies on carbon nanotube (CNT) breakdown current density, and the current-carrying capacity of single-walled CNTs (Ref. 6) is found to be on the order of 10^8 A/cm^2; in carbon nanofibers, the breakdown current density (J_{BR}) has been measured[7] to be around 5×10^6 A/cm^2. Electrical breakdown has been used to burn away successive shells in a multiwall CNT.[8,9] More recently, electrical breakdown has been used to obtain semiconducting CNTs from a mixture of CNTs since metallic ones burn away at a lower breakdown voltage.[10] Theoretical projections suggest that J_{BR} of graphene should be on the same order as for CNTs. However, little experimental evidence exists on the electrical breakdown of either 2D graphene or one-dimensional (1D) GNRs. In this work, it is experimentally shown that GNRs demonstrate an impressive J_{BR}. A simple relation between J_{BR} and nanowire resistivity is seen to emerge from the experimental data.

Few-layer graphene (one to five layers) is used as the starting material (see supporting material[11]). Each device consists of parallel ribbons fabricated between sets of electrodes, Fig. 1. The ribbon width between a pair of electrodes is designed to be the same for all the parallel ribbons. The range of widths studied in this work is 16 nm$<W<$52 nm, while the range of length is 0.2 μm$<L<$1.0 μm. 21 devices have been studied in this work, with each device yielding five to ten GNRs (depending on the overlap of patterned channels to few-layer graphene) between the middle electrode pair. The outer electrode pair is used to test for contact resistance (in a four-point probe setup). A semiconductor analyzer is used to apply a voltage ramp (at the rate of 50 mV/s) between the middle electrodes. Due to increasing current density in the GNRs, there is a voltage at which a GNR breaks down, resulting in a visible drop in current. The device testing is stopped at this point, and low bias measurements (for backgated resistance and contact resistance) are made. The voltage ramp is then repeated from 0 V. Successive GNR breakdowns occur at around the same voltage as for the first breakdown event. The breakdown current density of a GNR is extracted from the breakdown voltage and the resistance of the GNR; the resistance of a GNR for J_{BR} calculation is extracted from the difference in conductance immediately before and immediately after a breakdown event.

Figure 2(a) shows the *I-V* behavior of a device with 10 GNRs in parallel, and with $W=22$ nm and $L=0.75$ μm. The *I-V* curves are for a set of parallel GNRs—the top *I-V* curve is for ten GNRs in parallel, the second curve from top for nine GNRs in parallel, and so on. The *I-V* curve is initially linear and becomes saturated at increasing bias. This saturation is repeatable as the sample is cycled from 0 to 1.5 V; the contact resistance is found to be unchanged after bias cycling. This indicates that the nonlinearity at high bias is due to self-heating effects and not due to contact annealing. Such *I-V* saturation has been observed at high bias[12] in CNTs. Of the 21 devices tested in this work for breakdown current, 14 of the devices showed about a twofold increase in resistance (from low bias to the first breakdown event), six devices showed a 10%–20% increase in resistance, whereas one device showed no increase in resistance. The reason for this varying behavior could be twofold: (i) varying impurity den-

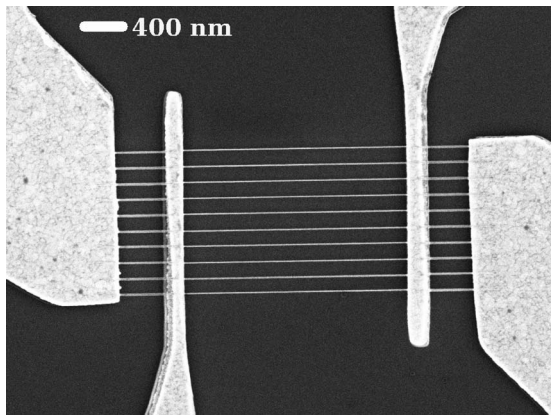

FIG. 1. SEM image of a set of ten GNRs between each electrode pair. The GNRs (below HSQ lines) are 21-nm-wide between the middle electrode pair.

[a]Electronic mail: raghu@gatech.edu. Tel.: 404 385 6463.

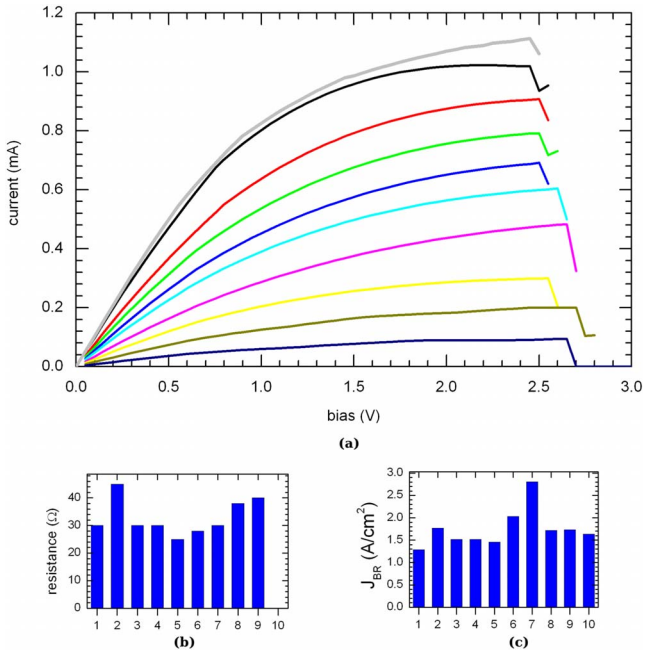

FIG. 2. (Color online) *I-V* curves of ten GNRs taken through electrical breakdown (a). Each GNR has a width of 22 nm and a length of 0.75 μm. The *I-V* curves are for a set of parallel GNRs—the top *I-V* curve is for ten GNRs in parallel, the second curve from top for nine GNRs in parallel, and so on. The testing is stopped immediately after a breakdown event, followed by low-bias measurements of contact resistance (b). The breakdown current density of the ten GNRs is plotted in (c) with the units of 10^8 A/cm^2.

sity between devices; the impurity density is estimated using the Dirac point shift[13] after contact metallization and is in the range $(2-19)\times 10^{11}$ cm^{-2}—a higher impurity density would cause more current saturation due to increased electron-phonon scattering and (ii) ballistic transport in short-length devices. It has been argued before[14] that ballistic transport (in CNTs) results in a linear *I-V* behavior with no current saturation at high bias. There are ten breakdown events for the device shown in Fig. 2(a), corresponding to the ten GNRs in the device. It is found from repeated low-bias measurements immediately after a breakdown event that 2–3 min is needed for a device to come back to its stable state from the self-heated state. Thus, low-bias measurements reported in this work are done 3 min after any previous high-bias cycling. Figure 2(b) shows the contact resistance after each breakdown event. The contact resistance is found to be almost constant after each event and is usually in the range of 30–80 Ω for the devices reported in this work. With a contact area of 0.5–1 μm^2, this translates to a contact resistance of 15–80 Ω μm^2. The breakdown voltage (V_{BR}) is seen to be around the same for all the ten GNRs in this device. Occasionally, it is seen that V_{BR} of a later breakdown event is smaller than that of the previous event. This may occur if the device has not fully reached its stable state from the previous high-current cycle. Figure 2(c) shows the breakdown current density of the ten GNRs—the range of current density is between 1.2 and 2.8×10^8 A/cm^2. The variation in current density could be because of a variation in the number of layers or impurity density variation.

Figure 3(a) shows breakdown current density of more than 100 GNRs versus their corresponding low-bias resistivity. A reciprocal relation is clearly seen between breakdown current density and nanoribbon resistivity (ρ). The best fit for

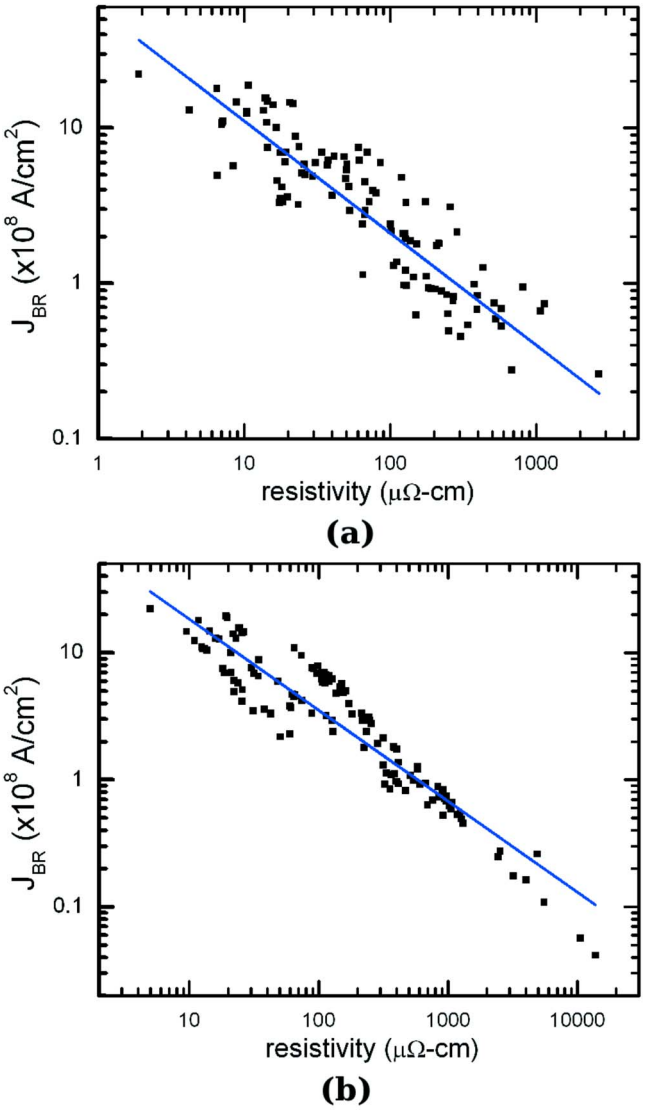

FIG. 3. (Color online) Breakdown current density vs resistivity; (a) shows a scatter plot with low-bias resistivity plotted on the *x*-axis—the R^2 for this fit is 74%; (b) shows a scatter plot for breakdown current density vs high-bias resistivity; the R^2 for this fit is 86%. The fit for both the plots is of the form $J_{BR}=A\rho^{-B}$ where $B=0.71$. If the breakdown mechanism was Joule heating, theory predicts that the exponent in the fit (b) should be 0.5; a steeper exponent in the fit indicates that the breakdown occurs faster for higher-resistivity GNRs, and might be indicative of higher defect densities contributing to faster electrical breakdown.

the data is obtained using the relation $J_{BR}=A\rho^{-B}$, where $A=5.72\times 10^8$, and $B=0.71$, with ρ having the units of $\mu\Omega$ cm; the R^2 for this fit is found to be 74.4%. Note that J_{BR} is extracted when the GNR is self-heated. The low-bias resistivity of a GNR, on the other hand, is extracted from the conductance difference between low-bias measurements done before and after a breakdown event. Figure 3(b) shows J_{BR} versus the high-bias resistivity (i.e., resistivity extracted from the conductance difference before and after a breakdown event). The best fit for the data is again obtained using the relation $J_{BR}=A\rho^{-B}$, where $A=9.57\times 10^8$ and $B=0.71$; the R^2 for this fit is found to be 86.2%. Using the 1D heat transport equation, a relation of the type $J_{BR}\propto 1/\sqrt{\rho}$ has been proposed.[15] The exponent of 0.71 extracted from the data suggests a faster breakdown with increasing resistivity; this indicates that the same factors that cause a higher resistivity also cause a degradation in breakdown current density, e.g.,

in-plane defects. For longer lengths, a relation of the type $J_{BR} \propto 1/\sqrt{(a\rho)}$ has been proposed,[7] where a is the cross-sectional area. Using a subset of data from Fig. 3(b) that have $L > 0.5$ μm, we get a fit (not shown) using the relation $J_{BR} = A(\rho a)^{-B}$ with $B = 0.55$; the fit has an R^2 of 92%.

It is possible to estimate the peak temperature in a GNR by solving the 1D heat transport equation[16]

$$V_{BR} I_{BR} \left[1 - \frac{1}{\cosh(L/2L_H)} \right] = gL(T_{max} - T_0), \quad (1)$$

where V_{BR} and I_{BR} are the breakdown voltage and current, respectively, g is thermal conductance of the GNR (to the substrate and top resist), L is GNR length, T_{max} is peak temperature in the GNR, and T_0 is the contact electrode temperature. Here L_H is the characteristic thermal healing length along the GNR and is given by $(ka/g)^{1/2}$, where k is thermal conductivity of the GNR. The relation can be rewritten as

$$g(T_{max} - T_0) = J_{BR}^2 \rho A \left[1 - \frac{1}{\cosh(L/2L_H)} \right]. \quad (2)$$

For an example GNR, $J_{BR} = 7 \times 10^8$ A/cm^2 and $\rho_{3D} = 100$ $\mu\Omega$-cm [Fig. 3(b)]. To evaluate T_{max}, it is necessary to assume values for g and k; from previously published results, $g = 0.20$ W/m K for bare CNTs on an oxide surface.[16] Previous measurements[17] on micron-wide, suspended graphene ribbons at room temperature yielded thermal conductivity values between 3080 and 5150 W/m K. Since the GNR has a thin HSQ layer on the top, this contribution has to be included as well; thus the value of g assumed above would need to be slightly higher than that found for bare CNTs on SiO_2. From Eq. (2), T_{max} is found to be 180 °C compared to 500–700 °C found for CNTs; if g is used as a fit parameter, even a low value of $g = 0.05$ W/m K results in a T_{max} of only 195 °C. It is unlikely that GNRs would breakdown at such low temperatures—indeed, it has been recently reported[18] that the peak temperature in the middle of a micron-wide single-layer graphene on SiO_2 is more than 700 °C. Thus, k is used as a fit parameter to obtain realistic values of T_{max}. For $k = 1100$ W/m K, 0.15 W/m K $< g <$ 0.30 W/m K results in a T_{max} between 700 and 800 °C. The thermal conductivity thus extracted—1100 W/m K—is for an 18-nm-wide ribbon. Similar calculations result in a thermal conductivity of 1000–1400 W/m K for other GNRs. Edge roughness scattering of phonons in graphene ribbons has been argued to result in a size-dependent thermal conductivity;[19] it is found that k at room temperature reduces from 5500 to 3000 W/m K as the width of a single-layer graphene ribbon is scaled from 9 to 3 μm. In addition, umklapp scattering[19] too reduces k as the temperature of a graphene ribbon is increased beyond about 100 K. Since the GNRs under discussion are both narrow and self-heated to temperatures of 700–800 °C, it is expected that both edge roughness scattering and umklapp scattering would play an important role in determining thermal conductivity.

In conclusion, GNRs are found to display an impressive current-carrying capacity of more than 10^8 A/cm^2 for widths down to 16 nm. The breakdown current density is found to have a reciprocal relationship to the nanowire resistivity and points to Joule heating as the likely mechanism of breakdown. The extracted thermal conductivity of sub-20-nm GNRs is more than 1000 W/m K.

The authors acknowledge funding support from Semiconductor Research Corporation/DARPA through the Interconnect Focus Center (IFC) and from Nanoelectronics Research Initiative (NRI) through the Institute for Nanoelectronics Discovery and Exploration (INDEX).

[1] C. Berger, Z. Song, X. Li, X. Wu, N. Brown, C. Naud, D. Mayou, T. Li, J. Hass, A. N. Marchenkov, E. H. Conrad, P. N. First, and W. A. de Heer, Science **312**, 1191 (2006).
[2] K. I. Bolotin, K. J. Sikes, Z. Jiang, M. Klima, G. Fudenberg, J. Hone, P. Kim, and H. L. Stormer, Solid State Commun. **146**, 351 (2008).
[3] M. Y. Han, B. Özyilmaz, Y. Zhang, and P. Kim, Phys. Rev. Lett. **98**, 206805 (2007).
[4] A. A. Balandin, S. Ghosh, W. Bao, I. Calizo, D. Teweldebrhan, F. Miao, and C. N. Lau, Nano Lett. **8**, 902 (2008).
[5] R. Murali, K. Brenner, Y. Yang, T. Beck, and J. D. Meindl, IEEE Electron Device Lett. **30**, 611 (2009).
[6] A. Javey, P. Qi, Q. Wang, and H. Dai, Proc. Natl. Acad. Sci. U.S.A. **101**, 13408 (2004).
[7] H. Kitsuki, T. Yamada, D. Fabris, J. R. Jameson, P. Wilhite, M. Suzuki, and C. Y. Yang, Appl. Phys. Lett. **92**, 173110 (2008).
[8] P. G. Collins, M. S. Arnold, and P. Avouris, Science **292**, 706 (2001).
[9] M. Tsutsui, Y. Taninouchi, S. Kurokawa, and A. Sakai, J. Appl. Phys. **100**, 094302 (2006).
[10] B. Gyoung-Ho, H. Jea-Ho, J. Eun-Kyoung, S. Hye-Mi, O. L. Jeong, K. Ki-jeong, and C. Hyunju, IEEE Trans. Nanotechnol. **7**, 624 (2008).
[11] See EPAPS supplementary material at http://dx.doi.org/10.1063/1.3147183 for material on fabrication and characterization techniques.
[12] P. G. Collins, M. Hersam, M. Arnold, R. Martel, and Ph. Avouris, Phys. Rev. Lett. **86**, 3128 (2001).
[13] Y.-W. Tan, Y. Zhang, K. Bolotin, Y. Zhao, S. Adam, E. H. Hwang, S. Das Sarma, H. L. Stormer, and P. Kim, Phys. Rev. Lett. **99**, 246803 (2007).
[14] P. Poncharal, C. Berger, Y. Yi, Z. L. Wang, and W. A. de Heer, J. Phys. Chem. B **106**, 12104 (2002).
[15] M. Suzuki, Y. Ominami, Q. Ngo, C. Y. Yang, A. M. Cassell, and J. Li, J. Appl. Phys. **101**, 114307 (2007).
[16] E. Pop, D. A. Mann, K. E. Goodson, and H. J. Dai, J. Appl. Phys. **101**, 093710 (2007).
[17] S. Ghosh, I. Calizo, D. Teweldebrhan, E. P. Pokatilov, D. L. Nika, A. A. Balandin, W. Bao, F. Miao, and C. N. Lau, Appl. Phys. Lett. **92**, 151911 (2008).
[18] M. Freitag, M. Steiner, Y. Martin, V. Perebeinos, Z. Chen, J. C. Tsang, and P. Avouris, Nano Lett. **9**, 1883 (2009).
[19] D. L. Nika, E. P. Pokatilov, A. S. Askerov, and A. A. Balandin, Phys. Rev. B **79**, 155413 (2009).